Electronic supplementary information for

Structure at air/water interface in the presence of phenol: A study using heterodyne-detected vibrational sum frequency generation and molecular dynamics simulation

Ryoji Kusaka,[a] Tatsuya Ishiyama,[b] Satoshi Nihonyanagi,[ac] Akihiro Morita,[de] and Tahei Tahara[ac]*

[a] Molecular Spectroscopy Laboratory, RIKEN, 2-1 Hirosawa, Wako 351-0198, Japan

[b] Department of Applied Chemistry, Graduate School of Science and Engineering, University of Toyama, Toyama 930-8555, Japan

[c] Ultrafast Spectroscopy Research Team, RIKEN Center for Advanced Photonics (RAP), 2-1 Hirosawa, Wako 351-0198, Japan

[d] Department of Chemistry, Graduate School of Science, Tohoku University, Sendai 980-8578, Japan

[e] Elements Strategy Initiative for Catalysts and Batteries (ESICB), Kyoto University, Kyoto 615-8520, Japan.

1. Snapshot of the present MD simulation

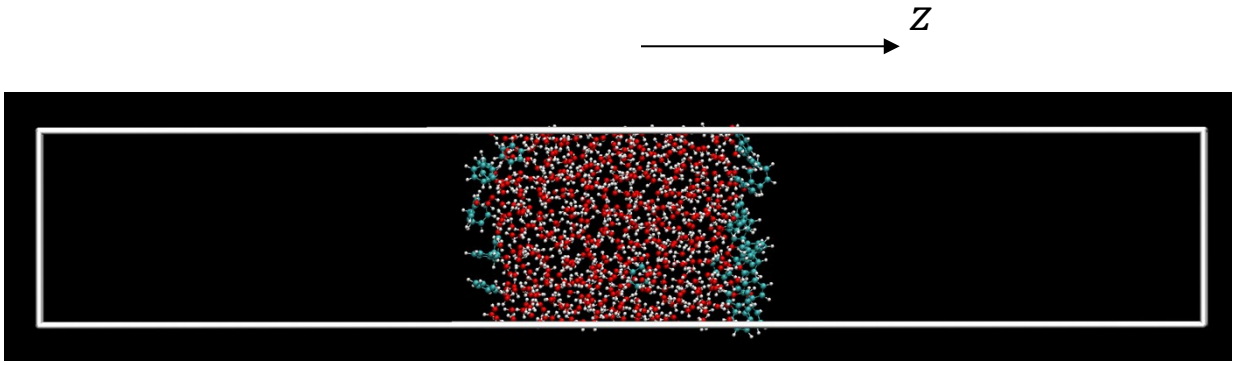

Fig. S1. A snapshot of the present MD simulation

2. SVD analysis

Fig. S2 shows the singular values obtained by SVD analysis of the four $\mathrm{Im}\chi^{(2)}$ spectra shown in Fig. 1 in the main text. The first and second components have large singular values, while the third and fourth components give nearly zero. This clearly indicates that the observed $\mathrm{Im}\chi^{(2)}$ spectra have only two predominant spectral components.

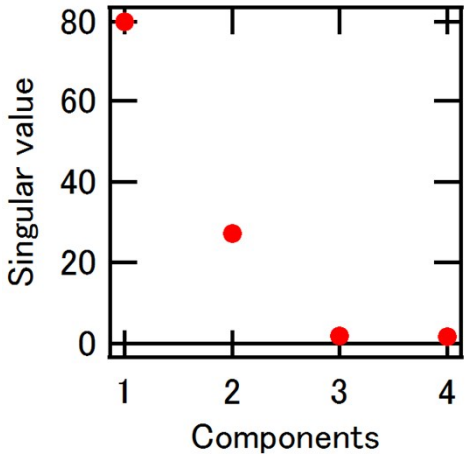

Fig. S2. Singular values obtained by SVD analysis of the four spectra shown in Fig. 1 in the main text.

3. Phenol in D_2O

Fig. S3 shows vibrational $Im\chi^{(2)}$ spectrum of the air/D_2O-phenol (117 mM) interface, in addition to that of the air/D_2O interface. Most of spectral features observed in the H_2O solution in Fig. 1 in the main text disappear in the D_2O solution, except for the negative sharp band at 3090 cm^{-1}. This observation means that the negative band at 3090 cm^{-1} is due to CH stretch of phenol and the rest of spectral features observed in the H_2O solution are due to OH stretches. The OH stretch of phenol can disappear in the D_2O solution spectrum because of the efficient H/D exchange with solvent. Additionally, the D_2O solution spectrum shows a weak positive band at 3030 cm^{-1}, indicating that this is due to another CH stretch of phenol.

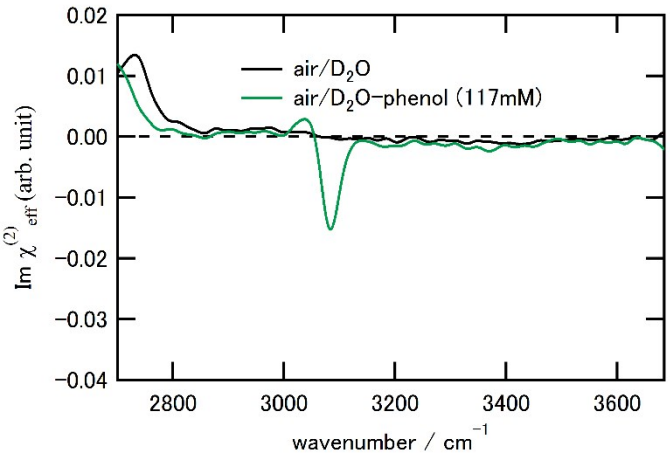

Fig. S3. Experimental vibrational $Im\chi^{(2)}$ spectrum of the air/D_2O-phenol (117 mM) interface (green) and that of the air/D_2O interface (black).

4. Relation between CH stretch $\chi^{(2)}$ and molecular orientation of phenol

As described in a previous study,[1] the second-order nonlinear susceptibility of symmetric OH stretch ($\chi^{(2)OH_{ss}}_{yyz}$) of water (C_{2v} symmetry) is related to its hyperpolarizabilities (β_{aac},β_{bbc},β_{ccc}), where the transition dipole moment of the symmetric OH stretch of water is set to be the direction of the c axis (Fig. S4). Since phenol is approximated as C_{2v} symmetry by considering the OH group to be a free rotor, $\chi^{(2)CH_{20a}}_{yyz}$ can be described in the same way as $\chi^{(2)OH_{ss}}_{yyz}$ of water as follows,

$$\chi^{(2)CH_{20a}}_{yyz} = \frac{1}{2}Ns\beta_{ccc}\langle cos\theta\rangle\left\{\left(\frac{\beta_{bbc}}{\beta_{ccc}}+\frac{\beta_{aac}\langle\cos^3\theta\rangle}{\beta_{ccc}\langle cos\theta\rangle}\right)\langle\cos^2\psi\rangle+\left(\frac{\beta_{aac}}{\beta_{ccc}}+\frac{\beta_{bbc}\langle\cos^3\theta\rangle}{\beta_{ccc}\langle cos\theta\rangle}\right)\langle\sin^2\psi\rangle\right\}$$

where *N*s is the number of surface phenol molecules and the brackets stand for ensemble average. The β_{aac},β_{bbc},β_{ccc} values of phenol were obtained by calculating the derivatives of the dipole moment and polarizability along the ν_{20a} coordinate using the Gaussian 09 program,[2] and it was found that the three hyperpolarizabilities are all positive. Because $\langle\cos^3\theta\rangle/\langle\cos\theta\rangle>0$, $\langle\cos^2\psi\rangle>0$, $\langle\sin^2\psi\rangle>0$, $\left(1-\frac{\langle\cos^3\theta\rangle}{\langle cos\theta\rangle}\right)>0$, and the observed $\chi^{(2)CH_{20a}}_{SSP}<0$, $\langle\cos\theta\rangle$ is negative. This means that phenol OH points toward the water phase.

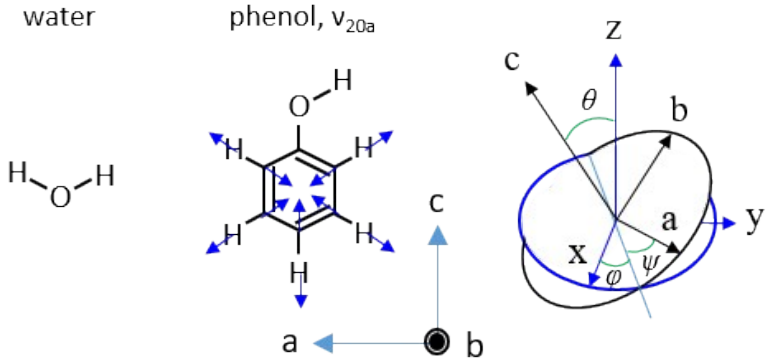

Fig. S4. Definition of the coordinates for phenol: molecular-frame coordinates (a, b, c), laboratory-frame coordinates (x, y, z), and Euler angles (θ, ψ, ϕ). z axis is the coordinate normal to the surface and points toward air.

5. Density profile

Fig. S5 shows the density profiles of water and phenol at the air/water-phenol interface obtained by MD simulation. $\hat{z}$ is the depth coordinate defined by $\hat{z} = z - z_{Gibbs}$, where z is the coordinate normal to the surface and z_{Gibbs} is the position of the Gibbs dividing surface. With this definition, $\hat{z} > 0$ refers to the air side and $\hat{z} < 0$ to the water side. Phenol (O), Phenol (C6), and Phenol (C.O.M) correspond to the oxygen atom, C6 atom defined in Fig. S6, and the center of mass of phenol, respectively. The density profile indicates that phenol is surface active and phenol OH points toward the water phase.

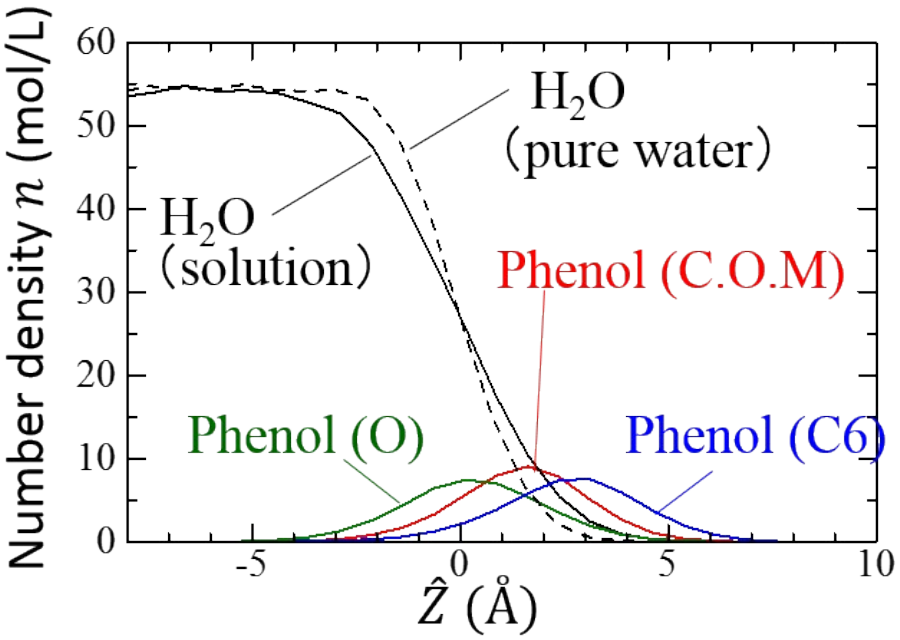

Fig. S5. Density profile of water and phenol at the air/water-phenol interface obtained by MD simulation.

6. Site number of phenol molecule

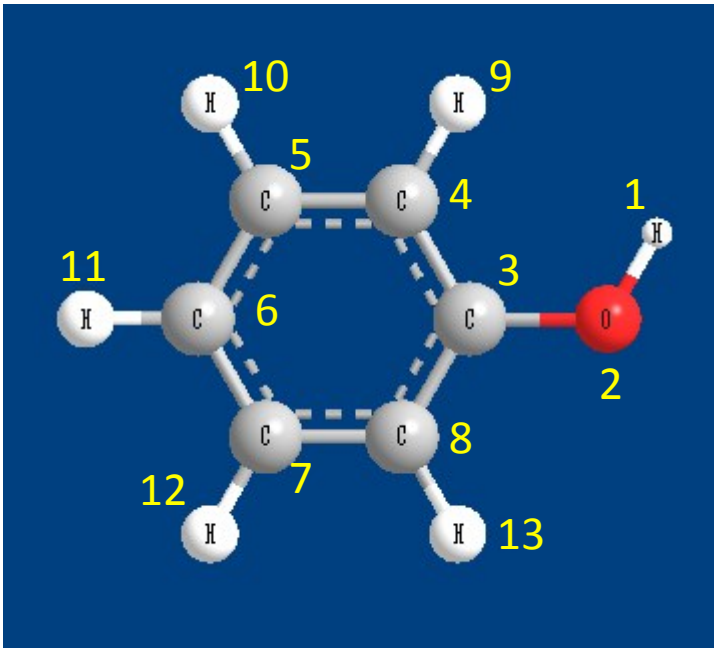

Fig. S6. Definition of site number of phenol molecule.

7. Comparison between the computed Im$\chi^{(2)}$ spectrum of the air/D_2O-phenol (C_6H_5OH) interface and the phenol OH component in the computed Im$\chi^{(2)}$ spectrum of the air/H_2O-phenol (C_6H_5OH) interface

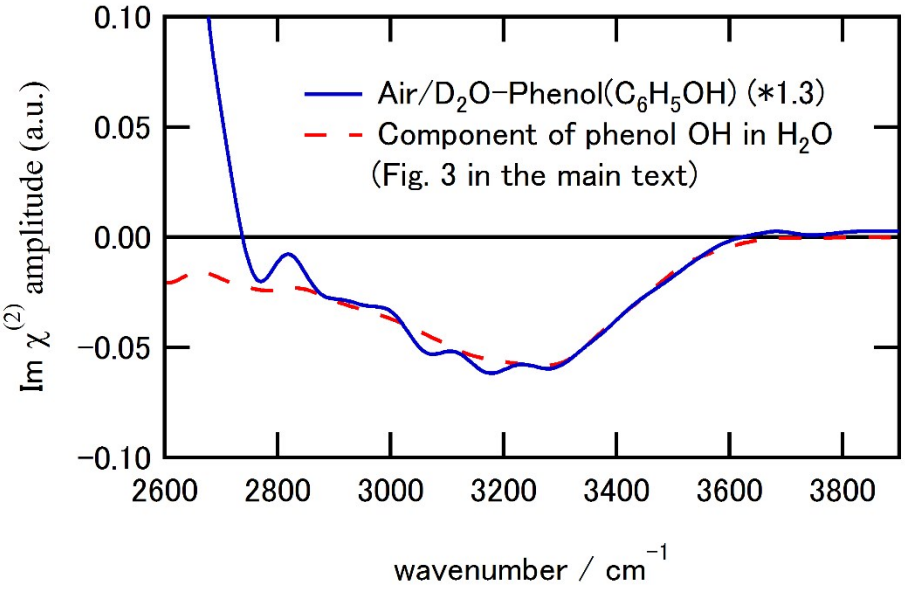

Fig. S7 Comparison between the computed Im$\chi^{(2)}$ spectrum of the air/D_2O-phenol (C_6H_5OH) interface (blue) and the phenol OH component in the computed Im$\chi^{(2)}$ spectrum of the air/H_2O-phenol (C_6H_5OH) interface shown in Fig. 3 in the main text (red broken).

Table SI. Intermolecular potential parameter k_n of phenol molecule (in a.u.) defined in Eq. (7).

$n=2$	3	4	5	6
0.2421	-0.8	0.8	-1.5	6.0

Table SII. Partial charge Q_a^{eq} of phenol molecule (in a.u.). See Fig. S6 for the numbering of phenol.

$a=1$	2	3	4	5	6	7	8	9	10	11	12	13
0.35499	-0.4678	0.14059	-0.09119	-0.20704	-0.12334	-0.18709	-0.02172	0.10047	0.14825	0.12965	0.12568	0.09855

Table SIII. CRK K_{ab}^{eq} of phenol molecule (in a.u.). See Fig. S6 for the numbering of phenol.

	$a=1$	2	3	4	5	6	7	8	9	10	11	12	13
$b=1$	-2.6644	2.70638	-0.39097	-0.05504	0.09996	0.14373	0.14761	-0.43034	0.43842	-0.05018	-0.02815	0.01813	0.06485
2	2.70638	-5.97474	3.53924	0.68188	-1.18419	-0.40981	-0.98351	1.04913	-0.5554	0.47872	0.6093	0.32247	-0.27947
3	-0.39097	3.53924	-7.06829	-0.1334	2.81179	-0.44192	2.43016	-0.0325	0.77151	-0.85332	-0.71786	-0.73058	0.81614
4	-0.05504	0.68188	-0.1334	-4.77786	-0.70039	2.04216	0.00458	1.73055	1.78637	0.90605	-0.48205	-0.54554	-0.45731
5	0.09996	-1.18419	2.81179	-0.70039	-5.00656	-0.30437	1.50938	-0.02319	0.91725	1.82234	0.92182	-0.32236	-0.54148
6	0.14373	-0.40981	-0.44192	2.04216	-0.30437	-4.98467	-0.29018	1.97422	-0.56112	0.79136	1.74525	0.78771	-0.49236
7	0.14761	-0.98351	2.43016	0.00458	1.50938	-0.29018	-4.7507	-0.6899	-0.49059	-0.34474	0.86336	1.71975	0.87478
8	-0.43034	1.04913	-0.0325	1.73055	-0.02319	1.97422	-0.6899	-4.7578	-0.40784	-0.52867	-0.47604	0.93082	1.66156
9	0.43842	-0.5554	0.77151	1.78637	0.91725	-0.56112	-0.49059	-0.40784	-2.40211	-0.25879	0.17325	0.423	0.16605
10	-0.05018	0.47872	-0.85332	0.90605	1.82234	0.79136	-0.34474	-0.52867	-0.25879	-2.27241	-0.27372	0.1311	0.45226

11	-0.02815	0.6093	-0.71786	-0.48205	0.92182	1.74525	0.86336	-0.47604	0.17325	-0.27372	-2.2693	-0.25764	0.19178
12	0.01813	0.32247	-0.73058	-0.54554	-0.32236	0.78771	1.71975	0.93082	0.423	0.1311	-0.25764	-2.23158	-0.24528
13	0.06485	-0.27947	0.81614	-0.45731	-0.54148	-0.49236	0.87478	1.66156	0.16605	0.45226	0.19178	-0.24528	-2.21152

Table SIV. The derivative of ^{Q_a} with respect to the internal coordinates $^{S = \Delta r_{OH}}$ of phenol molecule (in a.u.), $\partial Q/\partial S$. See Fig. S6 for the numbering of phenol.

$a =$ 1	2	3	4	5	6	7	8	9	10	11	12	13
-0.08328	0.08663	0.02491	-0.00202	-0.0124	0.00885	-0.0091	-0.01672	-0.00752	0.00304	-0.00502	0.00111	0.01152

Table SV. The derivative of $^{K_{ab}}$ with respect to the internal coordinates $^{S = \Delta r_{OH}}$ of phenol molecule (in a.u.), $\partial K/\partial S$. See Fig. S6 for the numbering of phenol.

	$a =$ 1	2	3	4	5	6	7	8	9	10	11	12	13
$b =$													
1	1.03024	-1.56116	0.27101	0.13464	-0.07682	-0.08844	-0.06942	0.22492	-0.09933	0.04554	0.08853	0.04915	0.05114
2	-1.56116	1.71061	0.12837	-0.08754	-0.13354	0.23384	-0.03211	-0.40762	0.19914	-0.0058	-0.07675	0.02731	0.00525
3	0.27101	0.12837	-0.67506	-0.07126	0.41285	-0.26355	0.16145	0.31946	0.01688	-0.10277	0.01358	-0.0925	-0.11846
4	0.13464	-0.08754	-0.07126	-0.23745	0.19146	-0.01826	-0.157	0.28101	0.16495	-0.05809	-0.03558	-0.03331	-0.07357
5	-0.07682	-0.13354	0.41285	0.19146	-0.47056	0.16215	0.09331	-0.41912	-0.03229	0.12793	0.00092	0.01567	0.12804
6	-0.08844	0.23384	-0.26355	-0.01826	0.16215	-0.1026	0.07204	0.1166	-0.01363	-0.04465	0.01713	-0.00399	-0.06664
7	-0.06942	-0.03211	0.16145	-0.157	0.09331	0.07204	-0.26015	0.13261	0.04638	-0.03401	-0.00889	0.06913	-0.01334
8	0.22492	-0.40762	0.31946	0.28101	-0.41912	0.1166	0.13261	-0.39368	-0.15263	0.12289	0.01158	0.00522	0.15876

9	-0.09933	0.19914	0.01688	0.16495	-0.03229	-0.01363	0.04638	-0.15263	-0.20575	0.01455	0.0095	0.02677	0.02546
10	0.04554	-0.0058	-0.10277	-0.05809	0.12793	-0.04465	-0.03401	0.12289	0.01455	-0.03992	0.00549	0.00052	-0.03168
11	0.08853	-0.07675	0.01358	-0.03558	0.00092	0.01713	-0.00889	0.01158	0.0095	0.00549	-0.01703	-0.01641	0.00793
12	0.04915	0.02731	-0.0925	-0.03331	0.01567	-0.00399	0.06913	0.00522	0.02677	0.00052	-0.01641	-0.04317	-0.00439
13	0.05114	0.00525	-0.11846	-0.07357	0.12804	-0.06664	-0.01334	0.15876	0.02546	-0.03168	0.00793	-0.00439	-0.0685

References

1. Nihonyanagi, S.; Yamaguchi, S.; Tahara, T., Direct evidence for orientational flip-flop of water molecules at charged interfaces: A heterodyne-detected vibrational sum frequency generation study. *J Chem Phys* **2009,** *130*, 204704.

2. Frisch, M. J.; Trucks, G. W.; Schlegel, H. B.; Scuseria, G. E.; Robb, M. A.; Cheeseman, J. R.; Scalmani, G.; Barone, V.; Mennucci, B.; Petersson, G. A.; Nakatsuji, H.; Caricato, M.; Li, X.; Hratchian, H. P.; Izmaylov, A. F.; Bloino, J.; Zheng, G.; Sonnenberg, J. L.; Hada, M.; Ehara, M.; Toyota, K.; Fukuda, R.; Hasegawa, J.; Ishida, M.; Nakajima, T.; Honda, Y.; Kitao, O.; Nakai, H.; Vreven, T.; Montgomery Jr., J. A.; Peralta, J. E.; Ogliaro, F.; Bearpark, M. J.; Heyd, J.; Brothers, E. N.; Kudin, K. N.; Staroverov, V. N.; Kobayashi, R.; Normand, J.; Raghavachari, K.; Rendell, A. P.; Burant, J. C.; Iyengar, S. S.; Tomasi, J.; Cossi, M.; Rega, N.; Millam, N. J.; Klene, M.; Knox, J. E.; Cross, J. B.; Bakken, V.; Adamo, C.; Jaramillo, J.; Gomperts, R.; Stratmann, R. E.; Yazyev, O.; Austin, A. J.; Cammi, R.; Pomelli, C.; Ochterski, J. W.; Martin, R. L.; Morokuma, K.; Zakrzewski, V. G.; Voth, G. A.; Salvador, P.; Dannenberg, J. J.; Dapprich, S.; Daniels, A. D.; Farkas, Ö.; Foresman, J. B.; Ortiz, J. V.; Cioslowski, J.; Fox, D. J. *Gaussian 09*, Gaussian, Inc.: Wallingford, CT, USA, 2009.